Control of sea-water intrusion by salt-water pumping: Coast of Oman

A. R. Kacimov · M. M. Sherif · J. S. Perret · A. Al-Mushikhi

Abstract A shallow alluvial coastal aquifer in the Batinah area of Oman, with sea-water intrusion that extends several kilometres inland, has been studied experimentally, analytically and numerically. The water table is proved to have a trough caused by intensive pumping from a fresh groundwater zone and evaporation from the saline phreatic surface. Resistivity traverses perpendicular to the shoreline indicated no fresh groundwater recharge into the sea. Using an analytical Dupuit-Forchheimer model, developed for the plain part of the catchment, explicit expressions for the water table, sharp interface location and stored volume of fresh water are obtained. It is shown that by the pumping of salt water from the intruded part of the aquifer, this intrusion can be mitigated. Different catchment sizes, intensities of fresh groundwater pumping, evaporation rates, water densities, sea level, incident fresh water level in the mountains and hydraulic conductivity are considered. SUTRA code is applied to a hypothetical case of a leaky aquifer with line sinks modeling fresh water withdrawal and evaporation. The numerical code also shows that pumping of saline water can pull the dispersion zone back to the shoreline.

Received: 10 March 2005 / Accepted: 8 December 2008
Published online: 20 February 2009

A. R. Kacimov (✉)
Department of Soils, Water, and Agricultural Engineering,
Sultan Qaboos University,
P.O. Box 34, Muscat, Al-Khod 123, Sultanate of Oman
e-mail: anvar@squ.edu.om

M. M. Sherif
Civil and Environmental Engineering Department,
United Arab Emirates University,
P.O. Box 17555, Al-Ain, UAE
e-mail: msherif@uaeu.ac.ae

J. S. Perret
Earth University, Guacimo,
Limón, Costa Rica
e-mail: jperret@earth.ac.cr

A. Al-Mushikhi
Ministry of Regional Municipalities,
Environment and Water Resources,
P.O. Box 323, Muscat, PC 113, Sultanate of Oman
e-mail: aziz_oman@yahoo.com

Keywords Coastal aquifers · Groundwater flow · Salt-water/fresh-water relations · Oman

Introduction

Al Batinah coastal plain, Sultanate of Oman, lies at the foot of the Western Hajar Mountains. After Muscat, the capital city, Al Batinah is the most densely inhabited area in Oman. It has been cultivated for many years with a variety of food crops. Figure 1 shows a map of Eastern Batinah (Oman) coastal catchments with wells and aflaj[1] (or *qanat* which are horizontal pipes that convey groundwater to the surface) monitoring sites, which were used for assessments of both subsurface and surface hydrological parameters. In Fig. 1, the contours of topographic elevation indicate the elevation (m) above the mean sea level (MSL), which ranges from about 500 to 2,500 m above MSL. Aflaj gauging stations are used to measure surface flow in open channels (wadis) that is generated by rare rains and continuous groundwater interception by the subsurface tunnels and springs. Unconfined coastal aquifers of the mapped catchments were studied by field, analytical and numerical techniques. More detailed hydrogeological data were collected and processed for Wadi Al-Maawel catchment.

Sea-water intrusion in coastal aquifers, as a natural process, is caused by a higher density and solute concentration of sea water and is exacerbated by extraction of fresh groundwater in overpumped catchments. Intrusion occurs as a saline 'tongue', which penetrates landward from the interface between sea water and the coastal aquifer (line SU_r in Fig. 2, which shows a vertical cross-section). The tongue propagation is stymied by fresh groundwater seeping to the sea from a higher elevation zone in the upper part of a coastal catchment. As a result, the tongue tapers in the landward direction with its toe (point D, Fig. 2) and tip (point A; Bear 1979). In steady regimes, standard models assume that groundwater is discharged into the sea through the beach window above the tongue. This window (in a cross-section) is a sea

[1] Aflaj (plural of falaj) is a channel system, which provides water for a community of farmers for domestic/agricultural use

 DOI 10.1007/s10040-008-0425-8

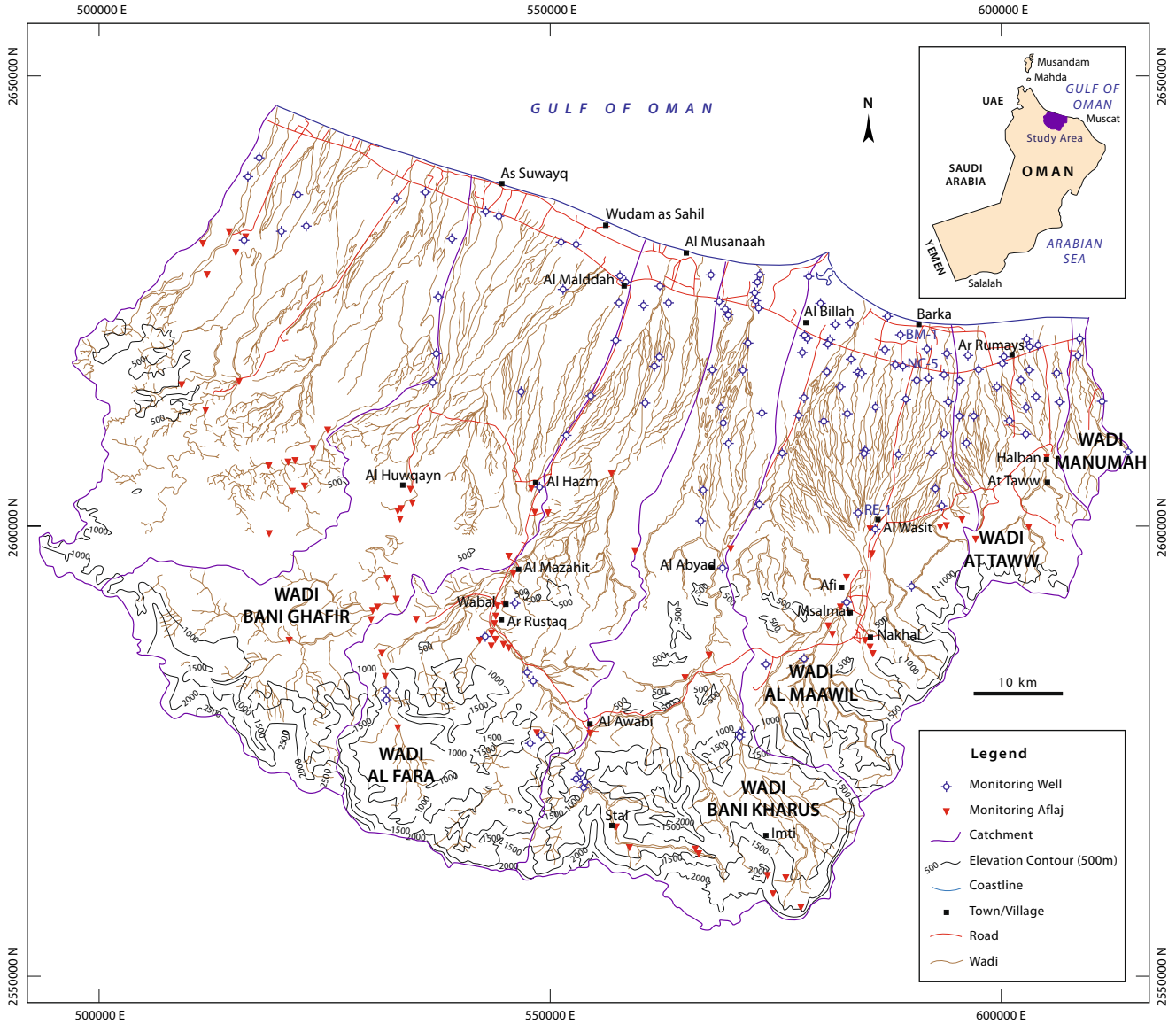

Fig. 1 Map of Eastern Batinah (Oman) coastal catchments. The contours indicate the topographic elevation above mean sea level (i.e. 500–2,500 m above MSL). *Red triangles* show the aflaj (qanat) gauging stations. *Black dots* show the monitoring wells

bottom line where the moving lighter fresh water contacts the hydrostatic heavier saline water. If the aquifer is unconfined, then a phreatic surface makes its own seepage face window (Fig. 9.20 in Bear (1979); Fig 7.31 in Strack (1989)) above the mean sea level.

Intrusion is characterised by EC (electrical conductivity) measurements in wells and by surface geophysical methods. EC of water samples is nearly linearly proportional to the ionic content or salinity. Induced and natural DC/AC (direct/alternating steady currents) or pulse-signals in geophysical surveying require further interpretation of high EC zones within the same hydrogeological unit as affected by intrusion.

Mathematical modeling is an efficient and inexpensive method of predicting intrusion (Bear 1979; Segol 1994; Strack 1989; Verruijt 1982). Two basic approaches in modeling are known, a variable density model (Voss 1984) and a sharp interface approximation. The former deals with the advective dispersion equation for solute transport. The latter, if applied in a homogeneous rock, solves the Laplace equation with a priori unknown free boundaries (interface and phreatic surface). If vertically averaged according to the Dupuit-Forchheimer (DF) concept, the free boundary problem is reduced to nonlinear partial and ordinary differential equations in a domain with two fronts, a tip and a toe (Bear 1979). Bakker (2003) extended the DF approximation to variable density flows by assuming several interfaces separating zones of constant density.

Numerous piezometric level isopleths obtained in the past (Al-Mushikhi 2002; Macumber 1998) show that in arid conditions and in intensively pumped catchments intrusion is different from the classical Ghyben-Herzberg type conceptual models, positing a net recharge to the water table and assigning the lowest phreatic surface point

 DOI 10.1007/s10040-008-0425-8

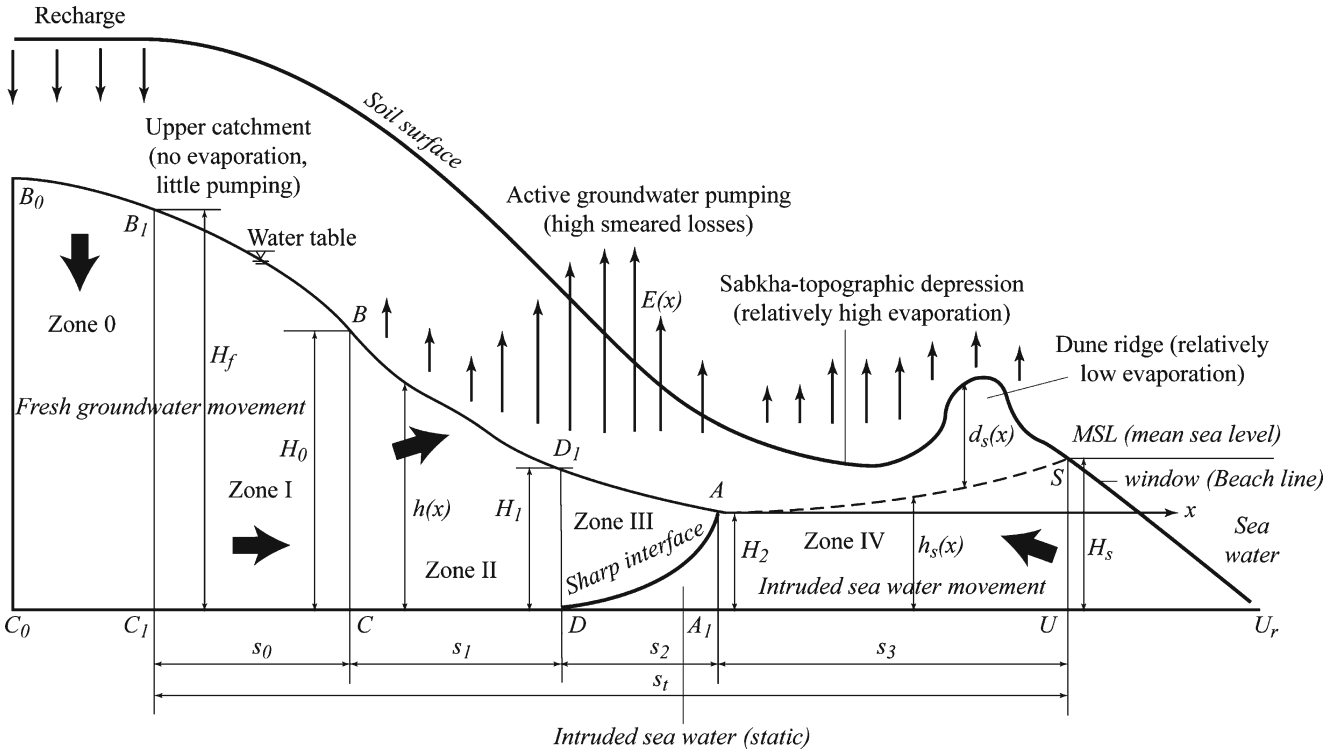

Fig. 2 Vertical cross-section of unconfined aquifer with indication of characteristic zones (*simple arrows* indicate losses from the water table and *block arrows* indicate groundwater movement directions). Terms are explained in the text

either at point S in Fig. 2 (the Dupuit-Frochheimer model) or above point S with a seepage face (a potential two-dimensional model; Bear 1979; Strack 1989).

In the near-shore zone of the study area (Fig. 2), a shallow water table bounds a sea-water-intruded trapezium, from which direct evaporation to the vadose zone and atmosphere occurs. These water table losses are especially pronounced in *sabkhas* (salt flats) where a clayey soil wicks moisture from the water table to a dry and hot surface (Yechieli and Wood 2002). Overall direction of sea-water seepage is inland. Fresh groundwater moves from the mountains to the sea but is intercepted by multiple wells. The fresh-saline water interface represents (on the catchment scale) a zone where two flows of different density meet. Thus, there is no hydraulic contact between fresh groundwater and the sea, i.e. no window of discharge through the beach surface exists.

Calvache and Pulido-Bosch (1997) also reported deep intrusion during the summer with no window that is caused by cyclostationary seasonal agricultural pumping in Spain. However, the aquifers studied in Spain still return to window-type conditions, i.e. with a direct discharge of fresh groundwater into the sea during winter when fresh water pumping drops. In the Oman case, the water table makes a persistent and deep regional trough with depressions of 5–9 m below MSL. This trough is located several kilometres inland from the shoreline and is roughly parallel to it. Since no signs of intrusion inversion (as in Calvache and Pulido-Bosch 1997) are detected in the Oman catchments, steady models of intrusion are used in the model.

An analytical DF model with an interface located far away from the coastal line is characterised by a triple point A (Fig. 2) where three different phases (fresh groundwater from the left, saline water from the right and vadose zone from above) meet (Kacimov et al. 2006). Mathematically, the interface AD has two fronts (triple point A and toe D). This flow regime degenerates into a window-type flow at small pumping rates and into a "dry gap" scenario (at extremely high water losses from AB and AS in Fig. 2).

A variable density numerical code SUTRA (Voss 1999) was also used to simulate intrusion in no-window conditions. For this purpose, the net extraction rate from the aquifer was modeled by smearing fresh-water consumption and saline water evaporation over line sinks on the top of a rectangular (in a vertical section) aquifer. The obtained quasi-interface is shown to propagate far inland. It corroborates qualitatively the full isolation of the sea from fresh groundwater that is predicted by the DF model.

The necessity to alleviate intrusion in Oman and United Arab Emirates (UAE) induced a spectrum of measures ranging from rationing of fresh-water abstraction to pumping of brackish water (Van Dam 1999; Sherif and Hamza 2001). Both the DF model and SUTRA predict that intrusion can be abated by smart saline water withdrawal. The pumped saline water is already used by desalination plants in Oman and Spain (Guhl et al. 2006), which reduce the production cost of water. The saline or brackish water pumped from the trapezium DASU in Fig. 2 can be also stored in recreational or fishery ponds from which water will evaporate. The relevant purpose of

 DOI 10.1007/s10040-008-0425-8

the investigation is to control sea-water intrusion by salt-water extraction but other engineering methods have been used in different countries to control sea-water intrusion (e.g. artificial recharge of waste water to form a barrier ridge, construction of subsurface dams).

In this paper, the following questions are answered: How do the intrusion and fresh water zone dimensions depend on: (1) abstraction rate of fresh water, (2) evaporation from the coastal zone, (3) soil and rock properties, in particular, the presence of *sabkhas*, (4) sea-water level and density, (5) fresh groundwater level in the mountains, (6) the size of the catchment, (7) the location and rate of saline water pumping?

General description of aquifers, catchments and intrusion

The Eastern Batinah (Oman) catchments and their unconfined aquifers were selected as representative examples of large-scale sea-water intrusion, Fig. 1. Catchment maps and satellite images are available (e.g. Al-Mushikhi 2002; Weyhenmeyer et al. 2002). For these catchments, the hydrological conditions, borehole salinity, TDEM (time-domain electromagnetic method) resistivity traverses, piezometric levels, lithology, hydrogeochemistry and other parameters are well documented (Al-Ghilani 1996; Al-Ismailiy 1998; Al-Mushikhi 2002; Al-Shibli 2002; Macumber 1998; Weyhenmeyer et al. 2002). A brief overview is presented here.

The study area consists of six surface catchments (total area of 5,400 km^2) within a strip of width 40–50 km, bordered in the north by the Gulf of Oman and in the south by the watershed of Jabal Al-Akdar and Nakhal mountains (elevations up to 2,000 m), which serve as a recharge zone to the coastal aquifers. The average salinity of sea water is 36,000 mg/L (average EC of 53,000 μS/cm) and its density ρ_s=1,030 kg/m^3; fresh water density ρ_f=1,000 kg/m^3. Precipitation varies from 60 to 180 mm/year in the coastal and highland parts of the catchments, respectively. The annual average surface (pan) evaporation rate in the coastal plain is 10 mm/day. The natural recharge from precipitation and agricultural irrigation return to the water table in the coastal part of the catchments are estimated to be between 2 mm/year in the coastal area and 54 mm/year in the mountains.

The hydrological balance in a representative Al-Maawil catchment of Batinah is characterised by 94 million m^3/year of annual pumping, which exceeds precipitation by 34 million m^3/year. The ensuing storage depletion occurs from two ends: water table drop and intrusion. For all six catchments, Al-Mushikhi (2002) showed that the annual balance of groundwater in 1999 was made up with 21% of sea-water intrusion as compared with 0.3% in 1973.

Hydrogeologically, the alluvial sequence consists of two hydrostratigraphic units, the total thickness of which reaches 600 m. The upper unconfined aquifer is a sub-recent and recent Quaternary alluvium. It has low clay content and high hydraulic conductivity ranging from 8 to 70 m/day (the average value is 20 m/day), transmissivity ranging from 1 to 500 m^2/day and a typical specific yield is 0.2. The water-table depth in the coastal zone is 1–10 m, and in the central plain and mountains it reaches 40 and 80 m, respectively. The type of groundwater varies from HCO_3–Ca–Na–Mg to Cl–Na from the mountains to the shore line. The lower ancient alluvium has much lower conductivity (1 m/day on average), thickness of 50–600 m and type of water HCO_3–Cl–Ca–Na–Mg. Although the deeper aquifer contains and conducts groundwater, only the upper aquifer, with an impervious bottom, will be considered below.

TDEM transects showed the resistivity of the upper aquifer in the range from 40 to 200 Ohm/m. The transition from fresh to saline (hypersaline) water in the boreholes is not smooth (EC profiles are sometimes oscillating with the blips allegedly reflecting small-scale rock heterogeneities). However, the final salinity maps (Macumber 1998), which are used by water managers, usually delineate the interface AD (shown as a curve in Fig. 2) as a tilted straight line.

Abnormally high EC values in boreholes are attributed not only to sea-water intrusion but also to the exudation of hypersaline connate water from a deeper marl formation. This extra-salinisation from deep sources was supposedly triggered by reduction of fresh-water pressure induced by intensive pumping from the upper aquifer. Similar results, a manifestation of intrusion, were obtained by on-ground TDEM surveys. In the near-shore line boreholes and dug wells (abandoned farms are plentiful in the Batinah) even the shallowest groundwater was high (sometimes close to that of sea water).

The Gulf of Oman is a regional discharge zone with a number of tectonic faults through which springs (in particular submarine ones) are routed. Piezometric levels have changed drastically during the last 30 years. In 1973 the MSL piezometric line coincided with the shore line, i.e. the window-type conditions of direct groundwater recharge through the beach zone held (Bear 1979). The 1993 triple point A (Fig. 2) advanced inland 5–20 km and the latest survey of intrusion (Al-Barwani and Helmi 2006) showed further increase of the intrusion zone with an extra 7% of agricultural land lost only in one inspected Batinah region. This was caused by the proliferation of electrical pumps and development of irrigation. For example, in the Batinah welayats (provinces) Sohar-Shinas-Liwa, for the total net crop area of 6,123 ha, the total number of wells was 20,195, according to the Ministry of Water Resources Aflaj Inventory completed in 2001. Similar overabstraction-intrusion scenarios have been observed in other hydrogeological systems (e.g. Salalah plain of Oman; Al-Shammas 2002). An atlas of water salinity in Oman was composed and published (MWR 1995). Groundwater over-exploitation, ensuing intrusion and the necessity to rectify salinisation are identified as a national priority for Oman.

To combat intrusion, several water management and engineering measures have been implemented. In particular, the Omani Government enforced a strict policy of

 DOI 10.1007/s10040-008-0425-8

well licensing. Recharge dams constructed since 1985 (three in the study area, 31 in the whole country as of 2007) and designed for runoff interception have proved to be effective means in creating temporary high values of fresh-water hydraulic head in critical zones. However, the salinity survey in the Batinah in 2005 showed that intrusion is still progressing at an alarming pace.

In order to understand better the scope of intrusion, six deep wells (500 m) were drilled in 2003 in Wadi Fara catchment, with an average distance of 20 km from the shore line. The borehole EC logs of these and other wells in the upper part of the catchments showed no signs of sea-water intrusion. Closer to the shore line, downhole geophysics detected the resistivity rise from 1,600 μS/cm in the shallow part of the aquifer to 50,000 μS/cm at depths of 30–120 m.

Near-shore resistivity mapping was conducted in 2003–2005 at Al-Hail site, Samail catchment by an OhmMapper instrument (Geometrics 2001) designed for shallow (up to 20 m) studies. A clear vertical resistivity gradient was established, indicating the presence of sea-water intrusion with a nearly horizontal saline water table and no fresh groundwater window. These geophysical profiles with transects parallel and perpendicular to the shore line corroborated the trapezium-shaped two-dimensional intrusion zone depicted in Fig. 2.

Upon completion of the OhmMapper studies, a pedon was dug 60 m from the shore line, reaching the water table AS in Fig. 2. The water table depth d_s (Fig. 2) was 1.8 m. Regular measurements of d_s and salinity during 2003–2005 in three installed piezometers showed that the water table is correlated with mild tidal and occasional post-rainfall variations and EC varied from 35,000 to 39,000 μS/cm. Therefore, direct measurements proved that the line AS in Fig. 2 is indeed a water table associated with saline conditions.

In the study area, the data on evaporation from the water table were assessed from the hydrological balance viewpoint and other records in the neighbouring sites (Al-Mushikhi 2002; Weyhenmeyer et al. 2002). Because the water table is relatively shallow in the near-shore part of the catchment, it was decided to study the properties of the vadose zone at the Al-Hail site.

Sieve analysis showed that the soil is a homogeneous sand of an average particle size of 0.26 mm and dry bulk density of 1.52 g/cm^3. The Rosetta Lite subpackage of HYDRUS2D (Simunek et al. 1999) predicted the saturated hydraulic conductivity of k=3.928 m/day while the Darcy column laboratory experiments gave 11 m/day. From Rosetta Lite the VanGenuchten parameters of the soil were retrieved as α=0.034, n=2.75, θ_s=0.37, θ_r=0.04 where θ_s and θ_r are the porosity and residual volumetric water content and α and n are the fitting constants in the Van Genuchten formula.

Measurements of the moisture content θ on the soil surface were regularly conducted in 2003–2004 by a θ−probe instrument (Delta-T Devices 2007) and by a TDR (time-domain reflectometer) probe. Both devices showed persistently constant values of θ in the range 0.02–0.05. Downhole TDR measurements in the installed boreholes showed that θ increases with depth from 0 to 1.8 m, exhibiting a distinct capillary fringe above the water table. The thickness of the capillary fringe monitored in the pedon and later in lab experiments conducted with repacked vertical columns was 40–50 cm. These results proved that the vadose zone in the study area satisfies the conditions of ultimate evaporation (Philip 1991), i.e. the ascending moisture flow from the water table to the ground surface is controlled not by atmospheric conditions but by the dry soil.

Steady-state evaporation from a horizontal water table to the soil surface was calculated by HYDRUS2D and the rate of loss from the water table (or evaporation flux), E_{s1}, was found to be 1.7×10^{-3} cm/day for this soil, surface moisture content and vadose zone thickness.

Next, field experiments were conducted in a *sabkha* site located 3 km from Al-Hail. In coastal sabkahs of Oman the capillary fringe comes to the soil surface. Correspondingly, evaporative loss can be high—up to 1 cm/day as reported by Yechieli and Wood (2002). Even if water under AS (Fig. 2) is a brine and evaporation is less than 2% of that for free water, the evaporation rate of 0.2 mm/day is close to the annual precipitation in the area (Wood and Sanford 2002). The water table depth at the *sabkha* site was ~2 m below the ground surface as at the Al-Hail site but the texture of the soil was completely different. In the *sabkha* profile, a visible fraction of salt crystals in the topmost 30–40 cm was detected. Two samples from a borehole were collected, one from the soil surface and another from a deeper point (2 m). The textural characteristics of the two samples were: (1) sand 11.31%, silt 36.96%, clay 51.72% (clay according to US Department of Agriculture); (2) sand 7.12%, silt 56.34%, clay 36.54% (silty clay loam).

Rosetta Lite of HYDRUS2D was used again. The VanGenuchten parameters were: α_1=0.0153, n_1=1.25, k_u= 20.71 cm/day; α_2=0.0153, n_2=1.25, k_l=12.13 cm/day (silty clay loam), where k is the hydraulic conductivity, α and n are the Van Genuchten parameters and subindexes "1", "u" designate the upper layer, subindexes "2", "l" stand for the lower layer of soil. The evaporation flux calculated by HYDRUS2D in this two-layer system is E_{s2}=2.04 mm/day, i.e. two orders of magnitude higher than E_{s1} at the Al-Hail site. Owing to omission of the salinity effect on evaporation in these simulations E_{s2} is significantly higher than the value reported by Wood and Sanford (2002) for Abu-Dhabi *sabkhas* in UAE.

If $d_s(x)$ in Fig. 2 is monotonic and the vadose zone soil is homogeneous, then $E(x)$ is a monotonically decreasing function (Kacimov et al. 2004) and for the depths of the water table more than 10 m, non-clayey alluvium evaporation can be neglected (Weyhenmeyer et al. 2002). However, the measurements and modeling reported above elucidated the necessity to count evaporation in shallow aquifers. A full hydrodynamic model for a two-layered aquifer with intensive evaporation from the water table was developed by Kacimov and Youngs (2005) but intrusion was not studied.

 DOI 10.1007/s10040-008-0425-8

Analytical solution for "natural" conditions

In this section an interface model is developed following the analysis of Youngs (2002) for constant (but different) water table losses in the fresh water and intruded sea-water parts.

Intrusion-related zonation is shown in Fig. 2. In the study area, an unconfined aquifer (an average saturated thickness of 50 m) overlies an impermeable layer C_0U_r, which is assumed to be horizontal (although the real aquifer bed is irregular, Kacimov 2006). In the DF model, pressure increases hydrostatically from the water table B_0B_1B D_1AS to C_0U_r (see Polubarinova-Kochina 1977, abbreviated as PK in what follows, and Strack 1989 for more details). The DF phreatic surface slope should be small. For zones 1–IV in Fig. 2, this limitation holds. For example, along a typical TDEM transect perpendicular to the shore line in Wadi Al-Maawel, the water table drops from 121.4 m MSL in well RE-1 located 21 km from the coast to –6.9 m MSL in well NC-5 (6 km from the coast) and –5.9 m MSL in well BM-1 (2 km from the coast).

Zone 0 ($C_0B_0B_1C_1$ in Fig. 2) is a regional recharge area where the water table is formed by infiltration from the fractured rock at high elevations. In the DF model, recharge intensity in the mountains can be assumed uniform because only exiguous data are available to estimate the spatial variability of rainfall. Rain gauging stations give pointwise records of precipitation (90–180 mm/year in Eastern Batinah). According to PK, the DF water table in uniformly infiltrated areas is an ellipse.

In zone 0, the rock data are scarce. In other zones of Fig. 2, there are pumping tests that provide information on the water table, hydraulic conductivity and aquifer thickness. In zone 0, the rock is fractured and karstified and little is known about its hydraulic properties. Moreover, the presence of springs here complicates the boundary conditions on the top of the saturated zone. The springs intercept water from perched aquifers, returning this water to wadis from where it seeps back to the subsurface.

In zone I (Fig. 2, C_1B_1BC), the recharge is relatively small and can be ignored. Evaporation is also set equal to zero because the depth of the water table from the ground surface d_s is high. The declivity is well pronounced but regular, unlike that in zone 0, where topography is ragged. Pumping is zero as it is not economical due to high d_s and relatively few water consumers.

The water table in zone I is a Dupuit parabola B_1B. The catchment-scale DF model starts from this zone. The height H_f is given and the location of C_1B_1 is fixed. In most coastal catchments of Oman, H_f is well recorded by the national network of observational wells. If climatic variations of precipitation are neglected then H_f is relatively stable, i.e. C_1B_1 is not affected by pumping, intrusion and other anthropogenic factors. In fact, this stability of the input boundary of the model is reinforced by the sloping nature of C_0U_r, i.e. the real topographic elevation of C_1 is well above D and A_1. The height H_0 in Fig. 2 is unknown and will be found from the mathematical solution below because H_0 depends on intrusion. However, the width s_0 of zone 1 (no-pumping zone) is known and fixed as it does not depend on intrusion.

Zone II in Fig. 2, $BCDD_1$, is subject to pumping for which the intensity is generally not uniform in space, i.e. depends on the x-coordinate in Fig. 2. Closer to farms and villages clustered in the plain, more water is consumed. If the losses from the water table in zone II are assumed to be x-uniform, then according to PK, the shape of BD_1 is a hyperbola. There is no sea-water intrusion in this zone. The right boundary of this zone is DD_1, the height of the water table there is H_1 and the length of zone II, s_1, is a priori unknown.

Zone III (DD_1AA_1 in Fig. 2) is bounded from above by the fresh-water table D_1A and propped by a sharp interface DA. Losses from the water table are due to pumping but the intensity of pumping diminishes in the coastal direction becoming nil at the triple point A because of the increasing problems with water quality. Although in the DF model the abstraction-evaporation losses are smeared over the x-coordinate and in Fig. 2 are shown as occurring from the water table, in reality pumping takes place from wells of finite screen lengths often located deep under the water table i.e. water is mixed within the borehole. In the DF model, individual wells can be taken into account if they are fully penetrating as, for example, in Strack (1989; pp. 104–108), but for the catchment scale model with hundreds of wells, it is not feasible to consider them individually, especially those wells for which pumping rates are not controlled. The right boundary of zone III is AA_1. The height of the water table there, H_2, and the length s_2 of zone III are to be found from the solution.

Zone IV in Fig. 2 (ADA_1US) is the sea-water intruded trapezium, two sides of which are curved. In zone IV the sloping nature of the beach is neglected i.e. instead of the real slope SU_r a vertical line SU as the right boundary is considered. This is common in the DF theory and the necessary corrections for tilted beaches can be done similarly to PK problems of seepage through trapezoidal dams where a triangular fragment, having a sloping boundary, is conjugated with a vertical face "core" fragment. Note that zone IV excludes the problem of matching boundary conditions between fresh and saline water on the beach surface (Kacimov and Obnosov 2001; Padilla and Cruz-Sanjulian 1997) because SU_r (SU) is a common constant head boundary.

The height H_s of sea water is known but the length s_3 of zone IV is not because point A is a front. It is emphasised that beneath the interface, i.e. in the curvilinear triangle DAA_1 the intruded sea water is stagnant although in A_1ASU it moves driven by evaporation. It is noted that D_1AS indeed makes a regional trough, i.e., the saline water table AS is dipping landward and the fresh-water table is dipping seaward. Obviously, there is no agricultural pumping in zone IV.

Stitching of DF-modeled zones I–IV in Fig. 2 is done by conjugating water tables and fluxes as in Strack (1989;

 DOI 10.1007/s10040-008-0425-8

pp. 82–86) with notations $h(x)$ and $h_s(x)$ for the fresh and saline water table elevations, respectively. Here, $h_f(x)=h(x)–H_s$ is also introduced. Both $h(x)$ and $h_s(x)$ are continuous everywhere and the slope of the water table is a continuous function everywhere but at point A. The flux of fresh (to the right) and saline (to the left) flows is continuous in all zones.

All seepage characteristics are related to a constant value of hydraulic conductivity, in particular, dimensionless losses $e=E/k$ are used. The dimensional discharge per unit length in the direction normal to the vertical plane related to k is Q. It is assumed that $e(x)=e_f$=const in zones II–III and $e(x)=e_s$=const in zone IV. Obviously, $0<(e_f, e_s)<\infty$.

For zone I there is a standard Dupuit expression for the flow rate

$$Q_f = \frac{H_f^2 - H_0^2}{2s_0} \tag{1}$$

All fresh groundwater in zones I–III is abstracted and consequently

$$Q_f = e_f(s_1 + s_2) \tag{2}$$

In zone IV (taking into account zero flux through AA_1),

$$s_3 = \sqrt{\frac{H_s^2 - H_2^2}{e_s}} \tag{3}$$

As has been shown by Van Der Veer (1977) and Kacimov et al (2006), in zone III both the water table D_1A and the interface DA are straight lines (this is true for E_f=const only) wherefrom

$$H_1 = s_2\sqrt{e_f(1+\delta)} \tag{4}$$

and

$$H_2 = s_s\delta\sqrt{e_f/(1+\delta)} \tag{5}$$

where $\delta = \rho_f/(\rho_s - \rho_f)$.

The condition along BC yields

$$(s_1 + s_2)\sqrt{e_f} = \sqrt{H_0^2 - H_s^2\delta/(1+\delta)} \tag{6}$$

The whole width s_t of the modeled part of zones I–IV is also known and fixed:

$$s_t - s_0 = s_1 + s_2 + s_3 \tag{7}$$

The seven equations above represent a system for seven unknown values of Q_f, H_0, s_1, s_2, s_3, H_1, H_2.

After some algebra, Eqs. (1)–(7) are reduced to two equations:

$$H_0^2 - H_s^2(1+\delta)\Big/\delta - e_f(s_1+s_2)^2 = 2e_f s_0(s_1+s_2) \tag{8}$$

$$H_s^2 - s_s^2 e_f \delta^2\Big/(1+\delta) = e_s(s_t - s_0 - s_1 - s_2)^2 \tag{9}$$

with respect to s_1 and s_2. Either s_1 or s_2 can be easily excluded from this system, after which one arrives at a standard quartic. Only one real root of the quartic has physical meaning. The "**Solve**" routine of *Mathematica* (Wolfram 1991) was used to find it for all dimensionless geometrical sizes related to H_s. The result is:

$$s_2 = \frac{1}{e_f\sqrt{\delta^3}}\sqrt{(1+\delta)\left(e_s + 2e_s s_t\sqrt{\delta e_f D} - \delta E\right)} \tag{10a}$$

$$s_1 = \frac{1}{e_f\sqrt{\delta}}\left(\sqrt{D} - \sqrt{\delta e_f}(s_0 + s_2)\right) \tag{10b}$$

where the following algebraic notations are introduced:

$$D = \delta\left(H_f^2 + e_f s_0^2\right) - (\delta + 1), \tag{10c}$$
$$E = e_s\left(H_f^2 - 1\right) + e_f\left(e_s\left(s_t^2 + s_0^2\right) - 1\right)$$

Although the quartic above is always solvable mathematically, the solution can violate the physical conditions in Fig. 2. In other words, the set of given physical parameters (H_f, H_s, δ, e_f, e_s, s_t, s_0) does not always give positive and properly limited s_1, s_2 and further s_3, H_0, H_1, H_2, Q_f. Namely, the flow pattern in Fig. 2 breaks at very high e_1, e_2, e_f values when, as Kacimov et al. (2004) showed, the fresh and saline water zones dwindle and eventually separate completely (dry gap between the intrusion tongue and groundwater tip). This is an extreme situation in this system where H_s ranges from 10 to 300 m. At these saturated thicknesses, even a very thin vadose zone in hyperarid conditions can not digest completely groundwater and create a hydraulic lacuna as in Kacimov et al (2004). A more practical regime when the zonation in Fig. 2 breaks, i.e. the flow pattern with a triple point does not exist, is the beach window scheme. Obviously, if e_f=0 and no fresh water is lost to the vadose zone and abstraction, then groundwater is doomed to discharge into the ocean.

In Fig. 3a, there are plots of s_1/H_s, s_2/H_s and $(s_1+s_2)/H_s$ as functions of e_f (curves 1–3) at H_f/Hs=1.2, δ=1/0.03, e_s=0.0001, s_t/H_s=20, s_0/H_s=2. It is important that in Fig. 3a $e_{fl}<e_f<e_{fu}$. The minimum e_{fl}, corresponding to the common window-discharge limit (point A in Fig. 2 drifts to the vertical beach), is found by Wolfram's *Mathematica* **FindRoot** from the equation $s_t - s_0 = s_2 + s_1$, i.e. s_3=0. For the case in Fig. 3 it gives e_{fl}=0.00104. The upper limit e_{fu} corresponds to a dry gap between the intruded sea water and seeping fresh water (point A descends to the bedrock and two "tongues" coming from the left and from the right

 DOI 10.1007/s10040-008-0425-8

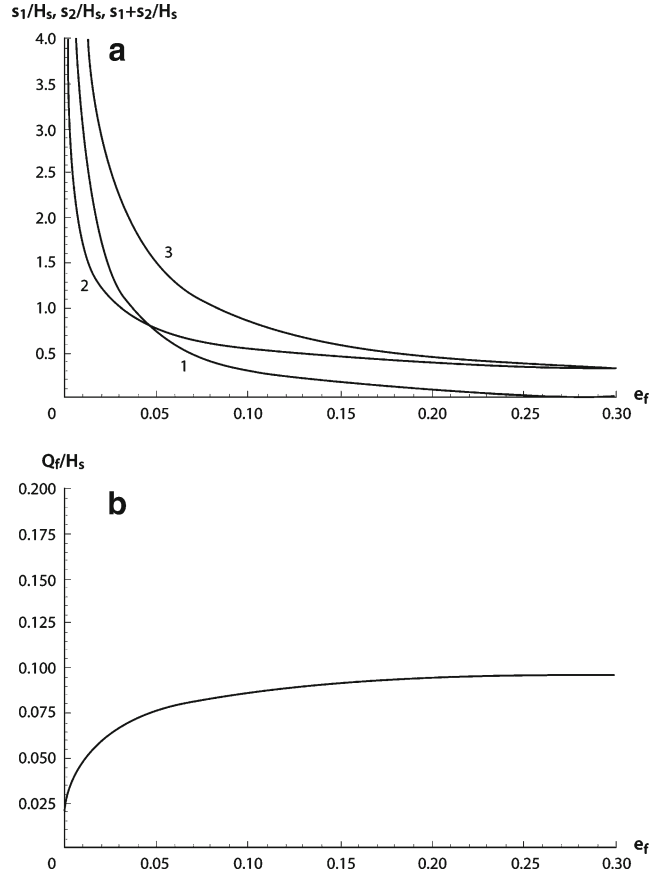

Fig. 3 Characteristic sizes of zones in Fig. 2: s_1/H_s, s_2/H_s and $(s_1+s_2)/H_s$ as functions of e_f (curves 1–3) at H_f/Hs=1.2, δ=1/0.03, e_s=0.0001, s_t/H_s=20, s_0/H_s=2 (**a**); fresh-water withdrawal rate $Q_f/H_s=e_f(s_1+s_2)/H_s$ as a function of e_f (**b**)

in Fig. 2 separate). From the equation H_2=0 it was found by *Mathematica* for the parameters in Fig. 3a that e_{fu}=0.302. As one can see from Fig. 3a intensification of fresh-water withdrawal results in a drastic decrease of the fresh-water zone, especially, at small e_f. Fig. 3b represents the curve of fresh-water withdrawal rate $Q_f/H_s=e_f(s_1+s_2)/H_s$ as a function of e_f. It is noteworthy that $Q_f(e_f)$ is nonlinear owing to $s_1(e_f)$ and $s_2(e_f)$.Any DF model should be tested against a full hydrodynamic sharp interface model of PK. This has been done (Kacimov et al. 2006) for a fragment including zones II–III in Fig. 2 and the DF results were in good agreement with the potential theory.

Analytical solution for "controlled" conditions

Integrated catchment-scale management of coastal aquifers should involve minimisation of intrusion. Mitigation of the shrinkage of the fresh-water compartment in the subsurface and associated dereliction of coastal agricultural farms on the surface is usually achieved by rationing and redistribution of fresh-water abstraction, i.e. by an optimal control of $E(x)$ in Fig. 2. It is intuitively clear that in order to minimise s_3 in Fig. 2 the distribution $E(x)$ in zone III should be appropriately managed. This is however an arduous task because of fuzzy water property rights intricately exacerbated by groundwater thefts, illegal well drilling, secret deepening of the boreholes, sabotage of centralised well water meters, etc.

A nontrivial method to combat sea-water intrusion was suggested by Sherif and Hamza (2001) who showed that pumping of the poor quality water from the dispersion zone can mitigate intrusion. This might seem paradoxical because increased water withdrawal causes an intensified seepage from the ocean i.e. more intrusion. In congruity with Sherif and Hamza (2001) it will be shown in this section that by controlling $E(x)$ in zone IV of Fig. 2 one can indeed reduce the size of the sea-water tongue. It is important that in zone IV nobody will object to pumping and using saline water. Water abstraction here is also relatively cheap because $d_s(x)$ (Fig. 2) is small.

A particular case of the general scheme in Fig. 2 is studied below with s_0=0, $H_0=H_f$. First, the simplest scenario of a piece-wise constant control of $E(x)$ in the saline water zone is tackled. Zone IV in Fig. 2 is divided into three zones IV–VI (Fig. 4) of widths p_1, p_2 and p_3. Obviously, $p_1+p_2+p_3=s_3$. Eventually, $s_1+s_2=p_f$ should be maximised. The distributed losses along the water table are set:

$$\begin{array}{llllll} e=e_f=const & in & zones & II & and & III \\ e=e_1=const & in & zones & IV & and & VI \\ e=e_2=const & in & zone & V, & e_2>e_1 & \end{array} \qquad (11)$$

Thus in zone V saline water is pumped (or a trench is constructed to which this water is drained and further evaporates). The x-smeared rate of losses e_2 there is higher than the rate of natural evaporation e_1 in zones IV and VI.

In order to solve the corresponding boundary-value problem, similarly to the previous section, AA_1 in Fig. 4 is set as a no-flow boundary and therefore zones IV–VI mathematically decouple from zones II–III. A new system of coordinates is originated at point A_1 with x-axis oriented rightward. According to the DF model the discharge potential Φ_d (Strack 1989) is introduced. This potential satisfies the governing equation

$$\frac{d^2\Phi_d}{dx^2}=e(x), \quad at \quad 0\le x\le s_3 \qquad (12)$$

where $\Phi_d=h_s^2(x)/2$ and $Q(x)=-d\Phi_d/dx$ is the corresponding discharge. Strack (1989; pp. 82–86) introduced the ditch function for localised infiltration (withdrawal), which makes it possible to obtain an overall solution of Eq. (12) in zones IV–VI by superposition of three functions, each of which satisfies the governing differential equation, and automatically guarantees continuity of flow. These functions, given as $G_0(x, \xi_1,\xi_2)$, where ξ_1, ξ_2 are dummy variables (Strack 1989), and defined throughout the domain $0\le x\le s_3$ satisfy automatically the condition of no flow at x=0.

 DOI 10.1007/s10040-008-0425-8

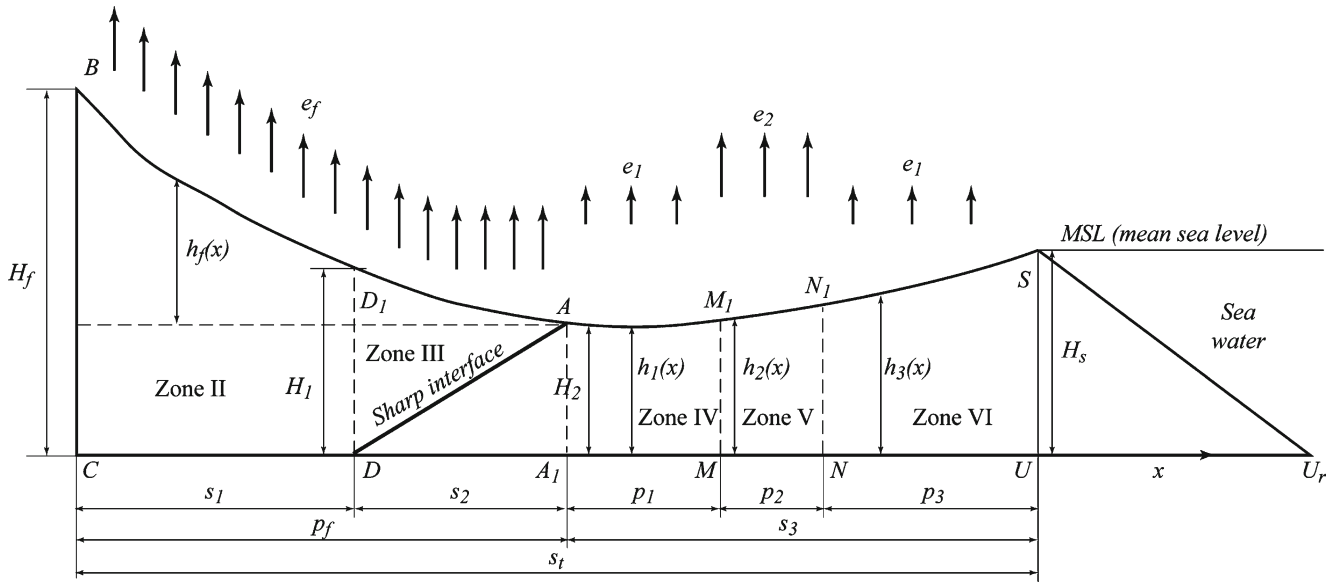

Fig. 4 Vertical cross-section with zonation for sea-water pumping scenario: free surface Dupuit-Forchheimer zonation

The solution obtained in this way by superposition is as follows:

$$\frac{1}{2}kh^2 = -e_1[G_0(x,0,p_1) + G_0(x,p_1,p_1+p_2)] - e_2G_0(x,p_1+p_2,s_3) + C_0, \quad (13)$$

where the constant C_0 is determined from the condition

$$\frac{1}{2}kH_s^2 = -e_1[G_0(s_3,0,p_1) + G_0(s_3,p_1,p_1+p_2)] - e_2G_0(s_3,p_1+p_2,s_3) + C_0, \quad (14)$$

which yields

$$C_0 = \frac{1}{2}kH_s^2 - e_1\left[\frac{1}{2}(p_1+p_2)^2 + p_1p_2\right] - e_2\left[p_2p_3 + \frac{1}{2}p_2^2\right] \quad (15)$$

The resulting phreatic surface is expressed as

$$h_1 = \sqrt{e_1x^2 + H_2^2}, \quad H_2 = \sqrt{H_s^2 - e_1\left(2p_1p_2 + (p_1+p_3)^2\right) - e_2p_2(2p_3+p_2)},$$
$$h_2 = \sqrt{e_2x^2 + 2(e_1-e_2)p_1x + H_s^2 + H_a},$$
$$h_3 = \sqrt{e_1x^2 + 2(e_2-e_1)p_2x + H_s^2 - (p_1+p_2+p_3)(2e_2p_2 + e_1(p_1+p_3-p_2))}$$
$$H_a = e_2\left(p_1^2 + 2p_1p_2 - p_2(2p_3+2p_1+p_2) - e_1\left(p_1^2 + 2p_1p_2 + (p_1+p_3)^2\right)\right. \quad (16)$$

In Eq. (16), the strip widths p_3 and p_2 are known, although p_1 and H_2 are not. Indeed, the interface AD, although straight, has two front points, A and D, whose location is a priori unknown. In order to find the unknown values of p_1, H_2, s_1 and s_2, the DF solution in zones II and III from Kacimov et al. (2006) is used. This solution gives for AD_1 a straight line:

$$h_f = -\sqrt{\frac{e_f}{(1+\delta)}}x \quad (17)$$

where, $h_f(x)$ is the fresh-water table elevation above the front point A (Fig. 4). For D_1B there is a hyperbola

$$\frac{1}{2}kH_s^2 = -e_1[G_0(s_3,0,p_1) + G_0(s_3,p_1,p_1+p_2)] - e_2G_0(s_3,p_1+p_2,s_3) + C_0, \quad (18)$$

which is conjugated with Eq. (17). From Eq. (18) for $p_f=s_1+s_2$

$$e_fp_f^2 = H_f^2 - H_2^2\frac{1+\delta}{\delta} \quad (19)$$

Now H_2 from Eq. (16) is put into Eq. (19). Remembering that $p_f+p_1+p_2+p_3=s_t$ one arrives at a quadric with respect to p_f. The positive root of this quadratic equation is:

$$p_f = \frac{1}{2(e_1+\delta e_1-\delta e_f)}\left[-2(1+\delta)s_te_1 + \sqrt{D_r}\right],$$
$$D_r = 4s_t^2e_1^2(1+\delta)^2 - 4(e_1+\delta e_1-\delta e_f)\left[(1+\delta)s_t^2e_1 - H_s^2 - e_1p_2^2 + e_2p_2^2 + 2p_2p_3(e_2-e_1) + \delta((H_f^2-H_s^2) + (e_2-e_1)p_2(p_2+2p_3))\right] \quad (20)$$

Thus Eq. (20) gives the location of the upper front point A as a function of the physical parameters e_1, e_2, e_f, δ, H_f, H_s, p_2, p_3 and s_t. Next, from the first Eq. (16), H_2 is

 DOI 10.1007/s10040-008-0425-8

calculated. From Eq. (17) the position of the second front point D is found from the equation

$$s_2 = \frac{H_2}{\delta}\sqrt{\frac{(1+\delta)}{e_f}} \tag{21}$$

and finally $p_1 = s_t - p_f - p_2 - p_3$.

As in the previous section, the problem parameters should be kept in certain limits to maintain the flow pattern in Fig. 4. First, e_f, e_1 and e_2 should not be too high. If they exceed a certain critical value, then a lacuna is formed as in Fig. 5a, i.e. the fresh and saline saturated zones become hydraulically disconnected. Second, H_f should be above a certain low bound (otherwise saline water will break through and reach BC). On the other hand, H_f should be below a certain upper bound. If H_f is too high (or, equivalently, the losses e_f are too small), then one arrives at the "no-window" flow pattern (Bear 1979) depicted in Fig. 5b. In this case, a saline phreatic surface has no chances to present itself to the vadose zone and the saline water tongue is completely submersed under the fresh-water zone.Now a parametric analysis of the regime in Fig. 4 will be presented. Fresh and sea-water densities are constant, and therefore, in all following examples, the value of $\delta = \rho_f/(\rho_s - \rho_f) = 1/0.03$ is fixed.

Effect of natural evaporation from the invasion zone

Natural evaporation E_1 is a hydrological parameter that depends on atmospheric conditions (air temperature and humidity, solar radiation, wind speed), soil properties (its dryness, capillarity and hydraulic conductivity) and the thickness $d_s(x)$ of the vadose zone. As the alaready discussed experiments and vadose zone modeling results showed, typical values of E_1 in zone VI are ~10^{-2} mm/day in sandy soils and ~10^{0} mm/day in *sabkhas* with corresponding dimensionless values of e_1 ~10^{-6} and ~10^{-2}.

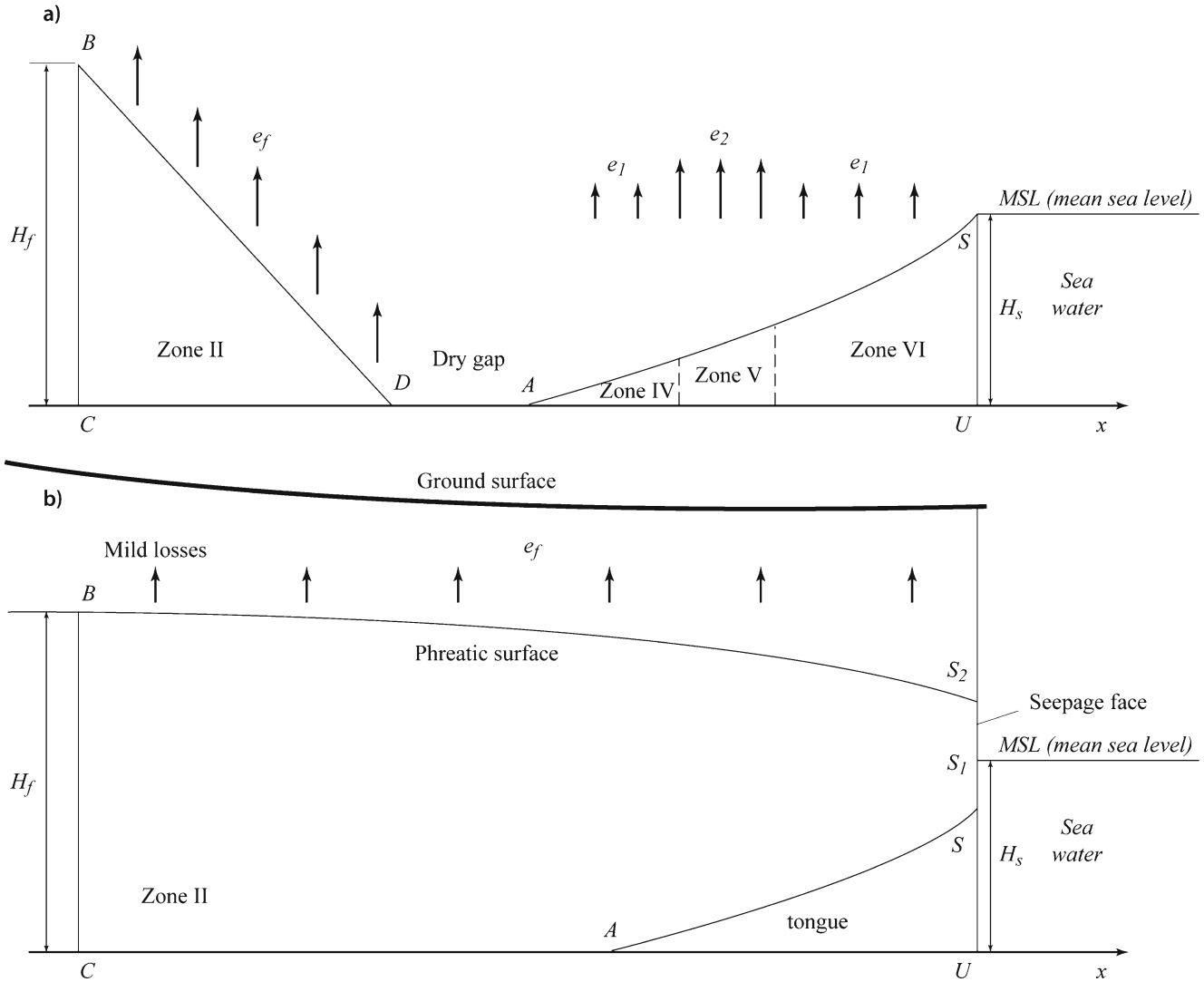

Fig. 5 Bounding flow regimes: **a** with a lost hydraulic contact between sea and groundwater, **b** beach "window" without the triple point

 DOI 10.1007/s10040-008-0425-8

The values H_f=70 m, H_s=50 m, s_t=10,000 m, p_2=10 m, p_3=10 m and e_2=0.1 were selected. In Fig. 6a, the curves $H_2(e_1)$ are plotted for three different intensities of water consumption in zones II–III: e_f=0.001, 0.002, 0.003 (curves 1–3). The upper limit of e_1 for the selected examples is e_{1c}= 0.00000325, 0.0000347, 0.000041, correspondingly. Figure 6b and c show the curves $p_f(e_1)$ and $s_2(e_1)$. As is clear from the graphs, the increase of e_1 results in the increase of p_f and decrease of H_2 and s_2. For example, at e_f=0.002 the value of p_f increases from 1,085 to 1,565 m.

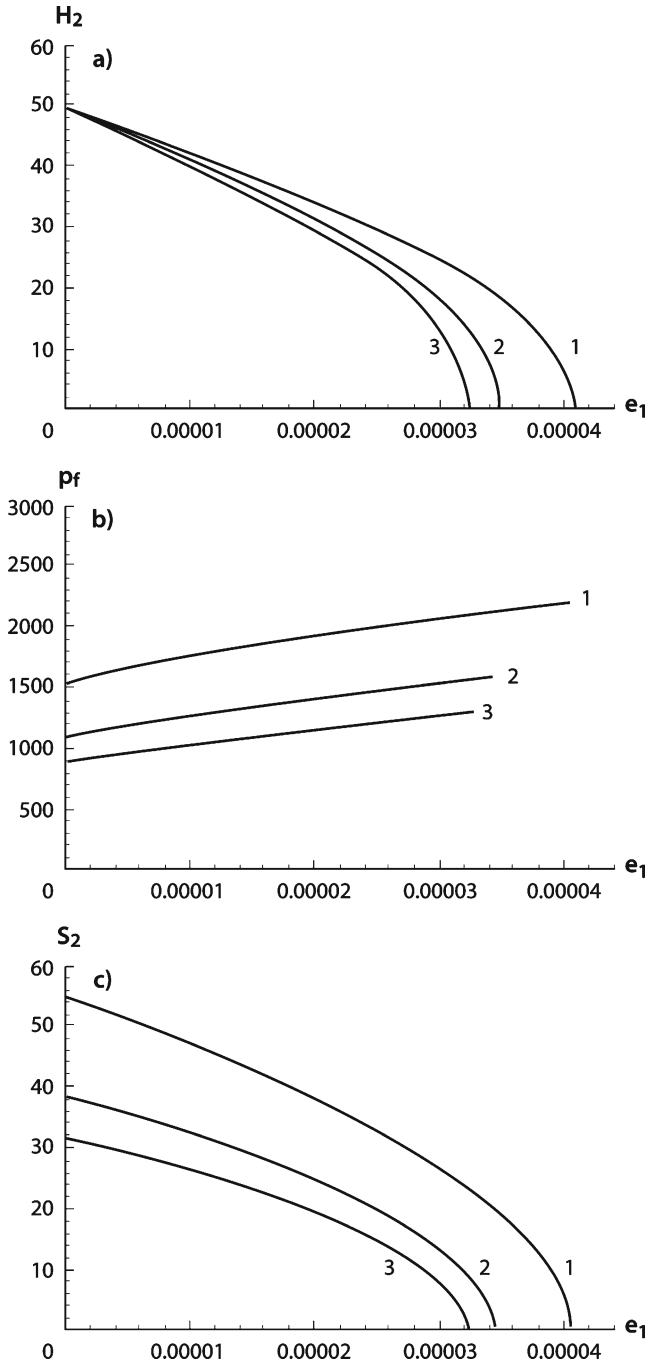

Fig. 6 Effect of evaporation rate from intruded saline water: **a** $H_2(e_1)$, **b** $p_f(e_1)$, **c** $s_2(e_1)$, for H_f=70 m, H_s=50 m, s_t=10,000 m, p_2=10 m, p_3= 10 m and e_2=0.1 and e_f=0.001, 0.002, 0.003 (curves 1–3)

Effect of saline water pumping

Zone V of artificially intensified losses from the encroached sea water can be controlled by engineering measures, i.e. one can increase abstraction e_2, relocate this strip or make it wider. The following parameters H_f= 70 m, H_s=50 m, s_t=10,000 m, p_2=10 *m,* e_1=10^{-5}, e_f=10^{-3} were kept. Fig. 7a shows $H_2(e_2)$ for three different distances p_3=100, 200 and 300 m (curves 1–3). Figure 7b presents $p_f(e_2)$ for the same values of p_3, while Fig. 7 illustrates that there is again a certain critical limit e_{2c} above which the whole flow pattern in Fig. 4 breaks into one in Fig. 5a. As one can infer from Fig. 7b, the relocation of the pumping strip from the shore line landward has an advantageous effect. Indeed, for a fixed strip width p_2 the same p_f is achieved at a smaller pumping intensity e_2 if p_3 is increased.

Effect of fresh-water abstraction

Fresh-water withdrawal of intensity e_f in zones II and III (Fig. 4) is the only adverse anthropogenic stress on the groundwater system. Practically, the rate of losses in m/s from the freshwater table, E_f, (or $k\,e_f$) is obtained by dividing

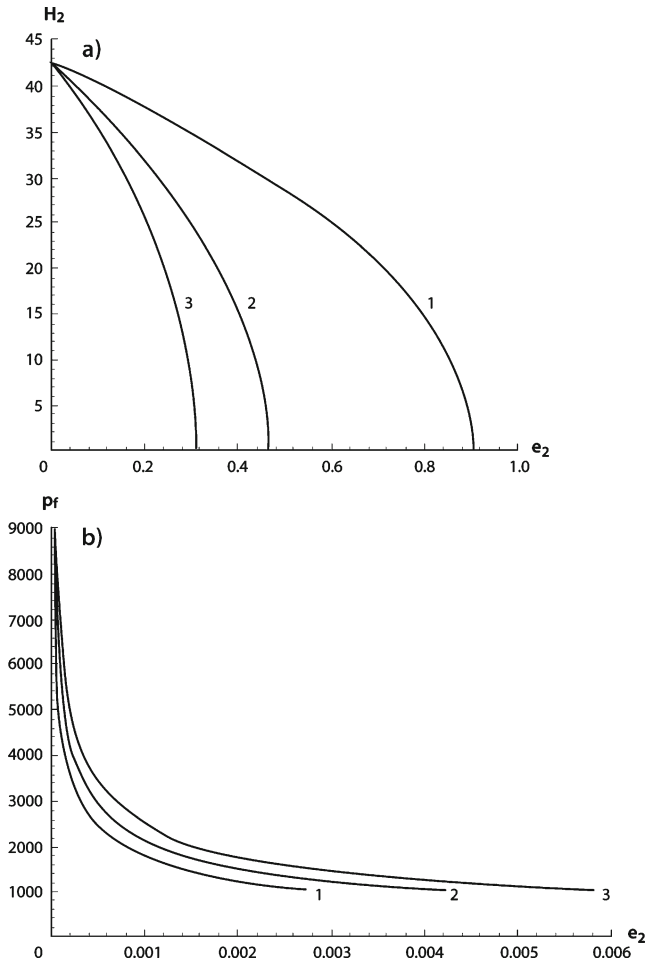

Fig. 7 Effect of saline water pumping rate: **a** $H_2(e_2)$, **b** $p_f(e_2)$ for H_f=70 m, H_s=50 m, s_t=10,000 m, p_2=10 m, e_1=10^{-5}, e_f=10^{-3} and p_3=100, 200 and 300 m (curves 1–3)

DOI 10.1007/s10040-008-0425-8

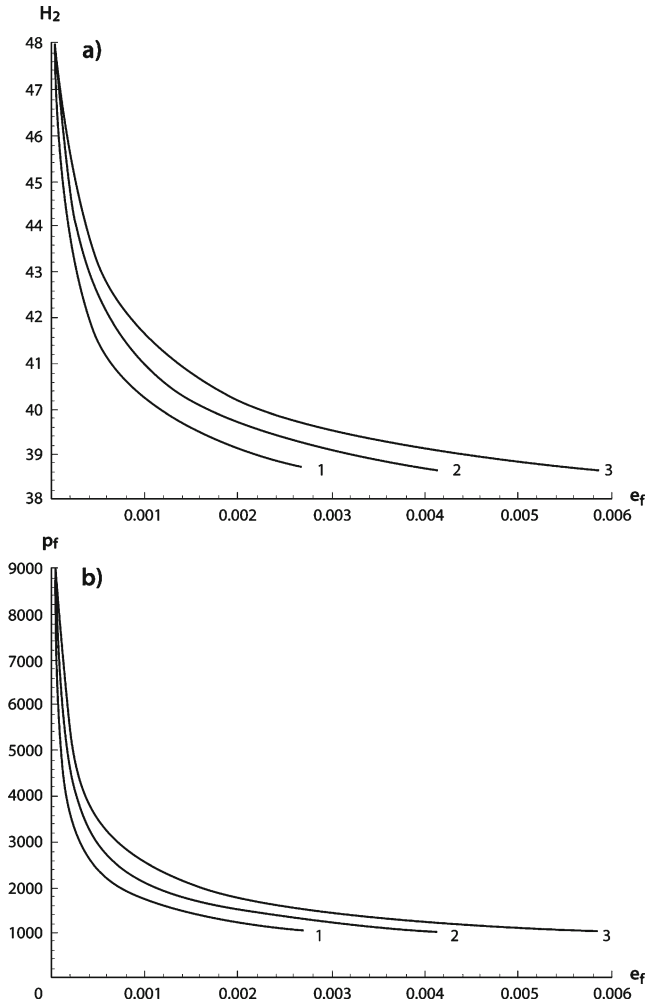

Fig. 8 Effect of fresh-water abstraction: **a** $H_2(e_f)$, **b** $p_f(e_f)$ for H_s= 50 m, s_t=10,000 m, p_3=100 m, p_2=10 m,e_1=0.00001, e_2=0.1 and H_f=70, 80, 90 m (curves 1–3)

the total flow rate of fresh water from all operating wells by the total catchment area. For example, the Salalah aquifer in Oman is characterised (Shammas 2002) by its plain area of Ar=825 km^2, and the daily use of groundwater by pumping is Q_{gw}=110,685 m^3/day. If one assumes no rainfall recharge in the plain area and no return infiltration from agricultural fields, then E_f=Q/Ar = 0.00013 m/day. This value is, most probably, much higher because E_f should be calculated for the area from point B to point A in Fig. 2, i.e. Ar is less than the whole catchment area. In the future, assessments of E_f can be improved if proper water metering in pumping wells is done and vadose zone infiltration under intensively irrigated areas is investigated. A typical value of E_f is at

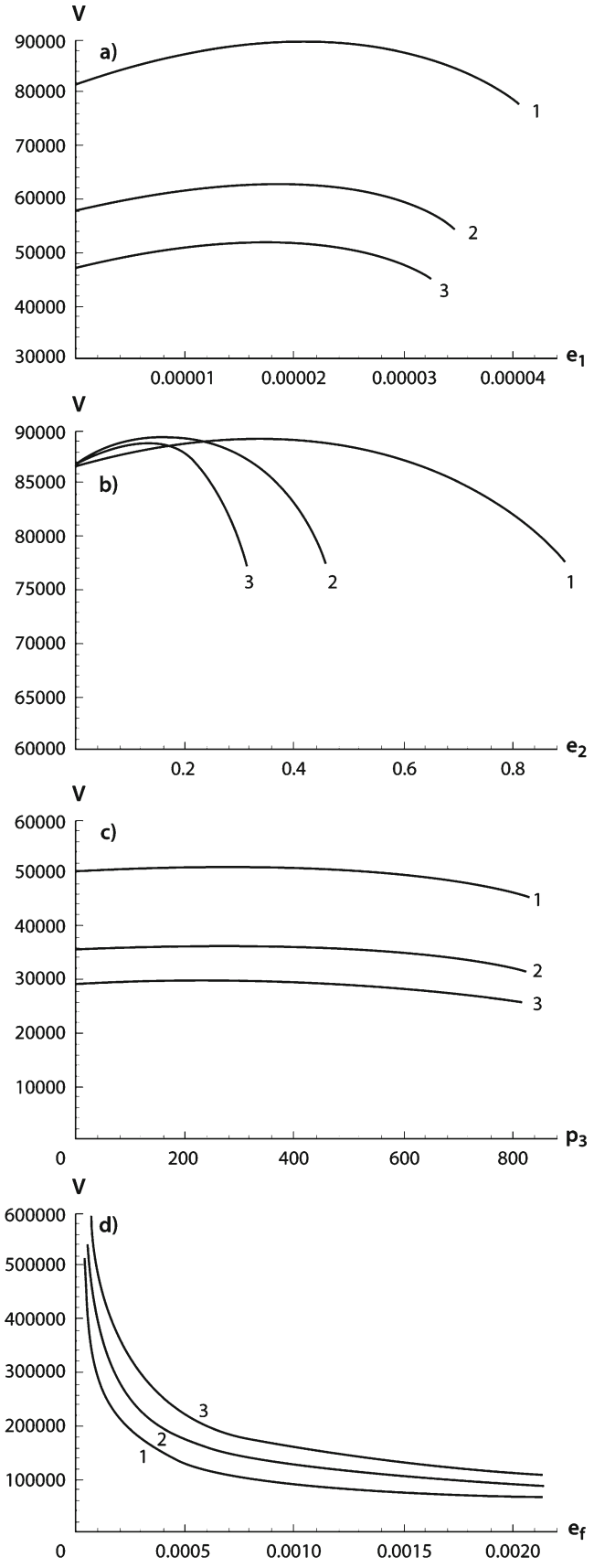

Fig. 9 Fresh-water volume (per unit length) **a** $V(e_1)$ for e_2=0.1, H_f= 70 m, H_s=50 m, s_t=10,000 m, p_2=10 m, p_3=10 m and e_f=0.001, 0.002, 0.003 (curves 1–3), **b** $V(e_2)$ for e_1=0.00001, e_f=0.001, H_f=70 m, H_s=50 m, s_t=10,000 m, p_2=10 m, and p_3=100, 200, 300 m (curves 1–3), **c** $V(p_3)$ for e_1=0.00001, H_f=70 m, H_s=50 m, s_t=10,000 m, p_2= 10 m, and e_f=0.003, 0.006, 0.009 (curves 1–3), **d** $V(e_f)$ for e_1=0.00001, e_2=0.1, H_s=50 m, s_t=10,000 m, p_2=10 m, p_3=100 m and H_f=70, 80, 90 m (curves 1–3)

 DOI 10.1007/s10040-008-0425-8

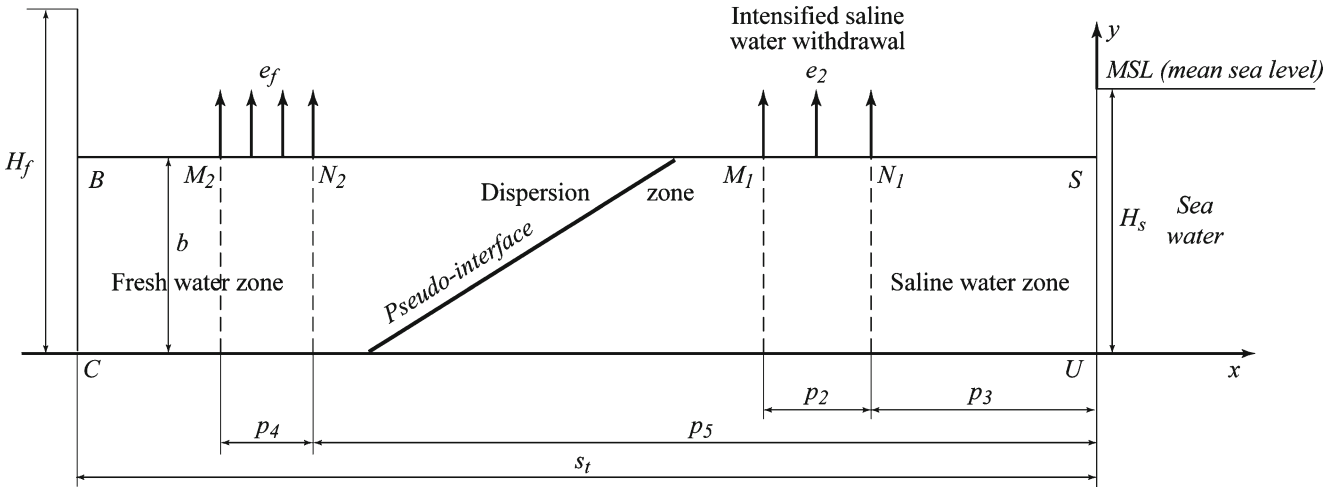

Fig. 10 Vertical cross-section considered in SUTRA model

least an order of magnitude higher than the direct rainfall-induced recharge to the water table, estimated as 2–5 mm/year (Al-Mushikhi 2002).

In computations the following parameters were fixed: H_s= 50 m, s_t=10,000 m, p_3=100 m, p_2=10 m, e_1=0.00001 and e_2=0.1. In Fig. 8a, $H_2(e_f)$ is shown at H_f=70, 80, 90 m (curves 1–3). From Fig. 8a, one sees that H_2 does not change much. By finding the critical values of e_f the inequality $e_{fl} < e_f$ was satisfied. The limit e_{fl} was determined as the maximum of e_{fl1} and e_{fl2} which were found by *Mathematica* as the roots of equations H_s=0 and p_1=0. The former equation was already discussed and the latter follows from the fixation of p_2+p_3. For the first curve (1) in Fig. 8a, e_{fl}=0.000026. The "dry gap" limit of Fig. 8a was not searched, i.e. e_{fu} was not found.

Figure 8b presents $p_f(e_f)$ for the same H_f as in Fig. 8a. From Fig. 8b one can see that p_f decreases severely with an increase of e_f. In order to rectify intrusion by a conventional rationing one should assess a particular catchment and understand which part of the $p_f(e_f)$ curve corresponds to a planned range of curtailing the fresh-water abstraction. Namely, strong nonlinearity of curves in Fig. 8b signifies that any apportionment of pumping at relatively high e_f will be much less effective than at small e_f. For example, the reduction of e_f in Fig. 8b from 0.001 to 0.0005 will result in a few hundred meters of increase in p_f; in order to enhance the fresh-water zone to kilometres one has to trim e_f to 0.0001, i.e. ten times.

Stored water volume

In coastal aquifers, intrusion is aggravated by dwindling fresh-water zones I–III, for which extension is demarcated by mountain watersheds, as shown in Fig. 2. It is therefore important to assess the remaining volume of water that

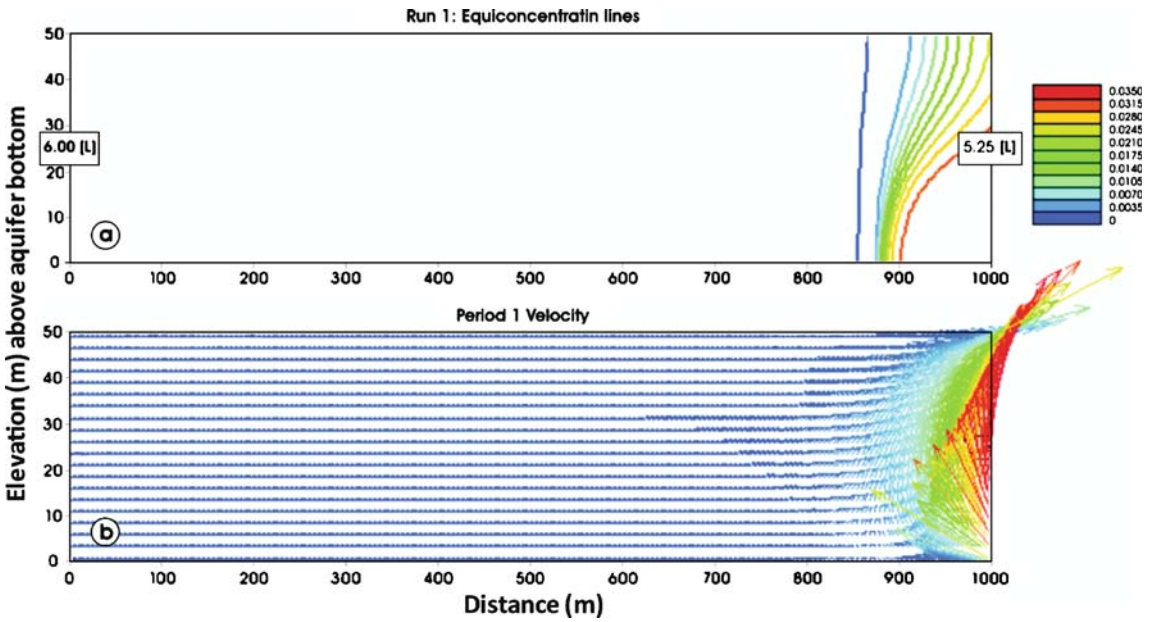

Fig. 11 SUTRA background modeling results, run-1: **a** equiconcentration lines, **b** velocity vectors

 DOI 10.1007/s10040-008-0425-8

can be mined/protected. In Fig. 4a, this volume (per unit length of the catchment in the direction normal to the vertical plane in Fig. 4a is equal to the area V_v (m^2) of voids in BCDAB. Remembering that DA is a straight line, one expresses $V=V_v/m$ (m is porosity) as

$$V = H_2 p_f - \frac{H_2 p_f}{2} + \sqrt{\frac{e_f}{1+\delta}\frac{l^2}{2}} + \int_{-p_f}^{-s_2} \sqrt{e_f x^2 + H_2^2(1+\delta)\delta}\,dx \qquad (22)$$

Using a built-in routine, **Integrate** of *Mathematica*, the integral in Eq. (22) was evaluated using Eqs. (16) and (20) explicitly (the expression for this integral is dropped here for the sake of brevity).

Figure 9a shows $V(e_1)$ plotted at e_2=0.1, H=70 m, H_s=50 m, s_t=10,000 m, p_2=10 m, p_3=10 m and e_f=0.001, 0.002, 0.003 (curves 1–3) with the upper bound of e_{1u} found as described above from the no-gap condition. For this set of parameters, there exists a value of the control variable e_1 at which V attains a global maximum. The corresponding V_m and e_{1m} were found by the **FindMinimum** routine of *Mathematica* as 89267.1 and 0.0000198604, 63121.4 and 0.0000173581, and 51538.4 and 0.0000163983 correspondingly for the three values of e_f. Figure 9b shows $V(e_2)$ plotted at e_1=0.00001, e_f=0.001, H_f=70 m, H_s=50 m, s_t=10,000 m, p_2=10 m, and p_3=100, 200, 300 m (curves 1–3). Although the extrema in Fig. 9a,b are rather mild, its very existence is non-trivial.

Figure 9c depicts the curves $V(p_3)$ plotted at e_1=0.00001, H_f=70 m, H_s=50 m, s_t=10,000 m, p_2=10 m, and e_f=0.003, 0.006, 0.009 (curves 1–3). From Fig. 9c, one can see that by relocating the saline water-pumping strip, a global maximum of V can be also reached. For example for the third (3) curve it is attained at p_3=220.12 m and the optimum is V_{max}=29,756 m^2.

The optima in Fig. 9a–c signify the intricate free boundary nature of the intrusion problem: the "horizontal" gain of fresh-water volume due to increased p_f can be nullified by decreased H_2 and ensuing tapering of AB (water table drop). Catchment-scale intrusion, if considered dynamically as transition from one e_f to another in Fig. 9a, takes place as a quasi-horizontal displacement (although AD is, of course, tilted) similarly to the rotational penetration of a sharp interface in a confined aquifer (Kacimov 2002). This is qualitatively different from those scenarios of "upconing" when overpumping drives saline water upward (Van Dam 1999) and hence, if reduced, results in recession and decay of the upconed interface. Unfortunately, in arid conditions of Oman, gravitational slumping of the interface, which occurs near a single well when pumping is stopped, can change only local salinity conditions. Only an overall catchment-wise control can palliate the invasion by displacing the corresponding trapezium in Fig. 2 back as a plug.

The discovered maxima in $V(e_1)$ and $V(e_2)$ graphs indicate that evaporation or pumping from the intruded trapezium increased above a certain limit can deplete the fresh-water zone despite the manifested retreat of the interface to the shore line. Consequently, one has to be cautious to hail a geophysical detection of the interface, pushed back to the shore line, as the only indicator of intrusion mitigation. The water table elevation in zones II–III should be monitored for a general assessment of the capacity of the whole groundwater compartment. Similarly, the retention dams creating temporary groundwater mounds should not be blandly commended because the interface geometry under the dam can have a shape of the Taylor-Saffman finger as in Kacimov (2001) rather than a fresh-water trapezium B_0C_0DA as in Fig. 2. Then the intruded sea water can be masked by the lens of infiltrated fresh water.

Figure 9d presents $V(e_f)$ plotted at e_1=0.00001, e_2=0.1, H_s=50 m, s_t=10,000 m, p_2=10 m, p_3=100 m and H_f=70, 80, 90 m (curves 1–3). These curves have a monotonically decreasing trend (recall that the total volume of fresh water abstracted is $Q_f=e_f p_f$). This decrease is highly nonlinear, quite contrary to linear pictures sketched by Van Dam (1999).

Fig. 12 SUTRA parametric analysis: acting head reduced by 5 m ▶ **a** equiconcentration lines (*run 2*), **b** equiconcentration lines (run 3), **c** equiconcentration lines (*run 4*), **d** velocity field (*run 4*), **e** equiconcentration lines (*run 5*), **f** velocity field (*run 5*)

SUTRA modeling

The main purpose of this numerical simulation is to examine the possibility of restoration of the groundwater quality in coastal aquifers by pumping saline (or brackish) groundwater from the area in the vicinity of the shoreline. SUTRA (Voss and Provost 2002) is a model for saturated-unsaturated, variable-density groundwater flow with solute or energy transport. It is an upgrade of the 1984 SUTRA computer code (Voss 1984). The code employs a two- or three-dimensional finite-element and finite difference method to approximate the groundwater flow and solute transport governing equations.

In order to demonstrate the effect of pumping of the intruded sea water from the coastal regions, an idealised vertical study domain of s_t=1,000 m in length and b=50 m in depth was considered, see Fig. 10. The porosity was set equal to 0.25. The layer was considered homogeneous but anisotropic. The horizontal permeability, k_x, was set equal to 10^{-6} m^2, while the vertical permeability, k_y, was set as 10^{-7} m^2. The dispersivities in the horizontal and vertical directions, α_L and α_T, were both set equal to 5 m. The other parameters were set as the default values of SutraGUI (Winston and Voss 2004).

The upper BS and lower CU boundaries in Fig. 10 are impermeable for water and solutes with the exception of two strips M_1N_1 and M_2N_2 through which relatively fresh and relatively saline water, respectively, is pumped. Along BC the fresh-water hydraulic head H_1=6 m. At SU the sea-water hydraulic head H_2=4 m.

DOI 10.1007/s10040-008-0425-8

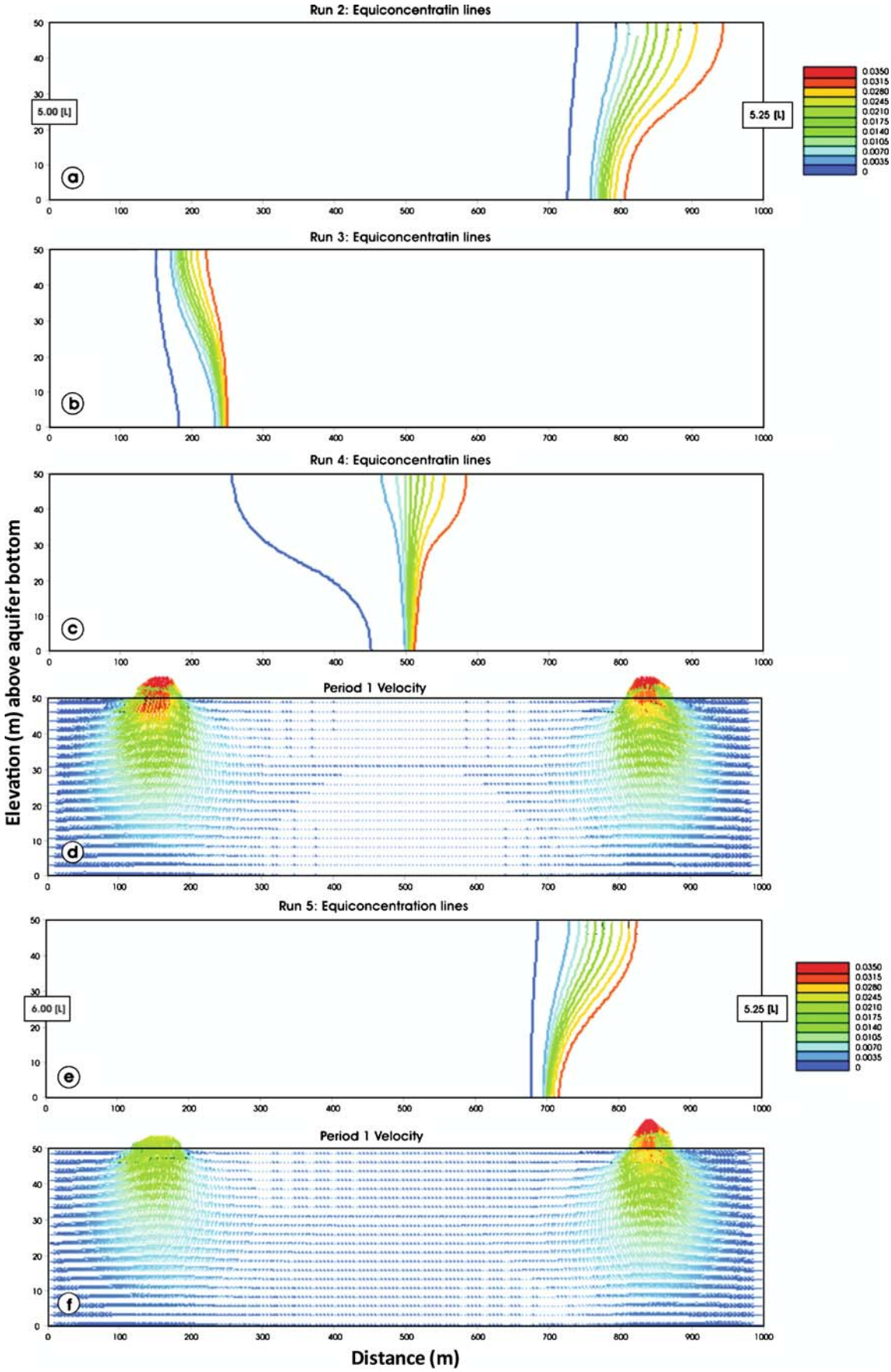

 DOI 10.1007/s10040-008-0425-8

However, this head was recalculated into an equivalent freshwater head (Sherif et al. 1988) h_{SU} as

$$h_{SU} = 4.0 + (50 - y)/\delta \quad (23)$$

where y is the elevation (m) of the nodal point above CU and δ=40. From Eq. (23) the maximum of h_{SU}= 5.25 m is at point U.

The study domain was discretised using the Fishnet tool (Winston and Voss 2004). The length of the domain was divided into 200 equal intervals each with a length of 5.0 m, while the depth was divided into 20 equal intervals each with a length of 2.5 m. In total, 4,000 rectangular elements (5.0×2.5 m) have 4,221 nodal points. All simulations were conducted under steady-state conditions.

In run-1 the SUTRA simulation was performed without any pumping to characterise the sea-water intrusion that would result due to the density difference between the freshwater and saline water bodies. The resulting equi-concentration lines are presented in Fig. 11a and the velocity vectors are presented in Fig. 11b. Benchmark equiconcentration lines 0.0 and 0.035, which represent the fresh and sea waters, migrated inland to a distance of 150 and 104 m, respectively, measured along the bottom boundary from the seaside. Meanwhile, a clear cyclic flow pattern is observed near the shoreline where the sea water intrudes the aquifer from the bottom and rotates back to the sea through the upper part of seaside boundary as brackish water.

In run-2, the specified head was reduced to 5.0 m and all other parameters were kept the same. The resulting equiconcentration lines are presented in Fig. 12a. The benchmark lines defining the width of the dispersion zone migrated inland to a distance of 277 and 196 m, respectively. As expected, reducing the hydraulic head at the land side increased the degree of intrusion and the width of the dispersion zone.

In run-3, the hydraulic head at the land side was maintained at 6.0. In addition a uniform freshwater pumping of 86.0 m^3/day was introduced through M_2N_2 with p_4=100 m and p_5=800 m (E_f=0.86 m/day). The benchmark lines moved inland to a distance of 820 and 754 m (Fig. 12b). It should be noted that these lines represent the final steady state conditions which might require a considerably long time to be achieved.

In run-4, in addition to the freshwater pumping (included in run-3), saline groundwater was also pumped uniformly at a rate of 86.0 m^3/day from a strip M_1N_1 with p_2=100 m and p_3=100. Figure 12c represents the resulting benchmark lines. These contours retreated toward the seaside and intersected the bottom boundary at a distance of 553 and 491 m, respectively. On the other hand, flow topology induced by two pumping strips created a zone of reduced velocity in between the strips that is depicted in Fig. 12d. Consequently, the width of the dispersion zone has increased near M_1N_1.

In run-5, the pumping of saline groundwater was increased to 130 m^3/day and all other parameters remained unchanged. Figure 12e and f present the resulting benchmark lines and velocity vector field in the study domain, respectively. The benchmark lines retreated more toward the seaside and the quality of the groundwater was enhanced considerably. The intrusion was mainly limited to the area between the sea boundary and saline groundwater pumping field. Despite the increase of total pumping of (fresh and saline) groundwater in runs 4 and 5, the overall quality of the groundwater in the aquifer has improved.

Conclusions

Sea-water intrusion in coastal unconfined aquifers of Eastern Batinah, Oman is investigated experimentally, analytically and numerically. Water table elevation, capillary fringe, moisture distribution, EC were observed and measured at a pilot site Al-Hail, Oman. Laboratory measurements of hydraulic conductivity and capillary rise were conducted in repacked columns in the laboratory. Evaporation from a shallow horizontal water table to a dry soil surface was modeled by HYDRUS2D.

These data were used in two catchment scale steady-state models of intrusion. The first DF model describes analytically a phreatic surface flow of fresh groundwater from highland and intruded saline water flow from the sea towards a regional trough generated by distributed losses from the water table. The losses simulate consumptive pumping from the fresh-water zone, evaporation from a shallow saline zone and artificial pumping of intruded sea water. The hydrodynamically balanced interface between fresh and saline water "hangs" with its toe on the impermeable underlying bed and a triple point where three free boundaries separating the fresh and saline water and vadose zone intersect. Sea water penetrates deep into the aquifer and groundwater has no hydraulic contact with the beach.

Mathematically, the solution in a particular case of a fresh groundwater zone without abstraction, which is adjacent to a constant intensity fresh-water withdrawal zone, and constant evaporation from the saline water zone is reduced to a simple quartic equation in which the solution is presented in an explicit form.

Another case is studied in which the fresh groundwater zone is under uniform abstraction but the saline water zone is exposed to both evaporation losses from the phreatic surface and distributed pumping along a near-shore strip. Explicit rigorous equations for the water table, flow rate and position of the interface are found. The required data include the width s_t of the plain part of the catchment, fresh-water table elevation H_f above an impermeable bed at the inlet of the plain, sea-water level H_s, densities of fresh and saline water ρ_f and ρ_s, intensity of fresh water pumping e_f, natural evaporation rate from a shallow near-coastal water table of intruded sea water, intensity of sea-water pumping e_2 from a strip of a width p_2 and the distance p_3 from this strip to the shoreline. The location of the interface AB in Fig. 2, the shape of

 DOI 10.1007/s10040-008-0425-8

the water table AD and the volume V of water stored in the fresh-water zone are calculated.

Analytical solutions have conditions of solvability, which mathematically bound the hydrogeological parameters and physically signify the transition from one regime to another. The regime focused on in this study (with a triple point) is demarcated by a classical regime where groundwater discharges through the beach slope and by a dry lacuna regime. In the latter, extraordinary high evaporation causes a hydraulic discontinuity between the intruded sea water and fresh groundwater bodies.

The second numerical model based on SUTRA assumes a rectangular confined aquifer with exfiltration line sinks placed along its top. These sinks simulate fresh-water abstraction, evaporation and saline water pumping similarly to the DF model. Circulatory movement of saline water is quantified near the beach. Pumping of saline groundwater from coastal aquifers would mitigate the migration of sea water deep into the aquifer and would contribute to the enhancement of the groundwater quality. This finding is consistent with the findings of Sherif and Hamza (2001).

Acknowledgements This study was supported by the joint Sultan Qaboos University -United Arab Emirates University project CL/SQU-UAEU/0/3/02. Comments of two anonymous reviewers are highly appreciated.

References

Al-Barwani A, Helmi T (2006) Sea water intrusion in a coastal aquifer: a case study for the area between Seeb abd Suwaiq, Sultanate of Oman. Agric Mar Sci 11:55–69

Al-Ghilani N (1996) Saline intrusion and groundwater recharge in the Al-Khoud fan, Sultanate of Oman. MSc Thesis, University of Wales, Wales

Al-Ismaily A (1998) Coastal aquifer mapping in Oman based on performance evaluation of DC resistivity and TDEM techniques, and the integration of geophysical methods. MSc Thesis, Delft Technical University, The Netherlands

Al-Mushikhi AAM (2002) Formation of subsurface water of the southeast Batinah region (Sultanate of Oman) and perspectives of development (in Russian). PhD Thesis, Moscow State Geoexploration University, Russia

Al-Shibli SH (2002) Modeling of saltwater intrusion in Wadi Al-Jizi aquifer. MSc Thesis, Sultan Qaboos University, Muscat, Oman

Bakker MA (2003) Dupuit formulation for modeling seawater intrusion in regional aquifer systems. Water Resour Res 39(5), 1131. doi:1029/2002WR001710

Bear J (1979) Hydraulics of groundwater. McGraw-Hill, New York

Calvache ML, Pulido-Bosch A (1997) Effects of geology and human activity on the dynamics of salt-water intrusion in three coastal aquifers in southern Spain. Environ Geol 30:215–223

Delta-T Devices (2007) Delta-T Devices, Cambridge, UK. http://www.delta-t.co.uk/. Cited December 2008

Geometrics Inc. (2001) Geometrics OhmMapper operation manual. Geometrics, San Jose, CA, USA

Guhl F, Pulido-Bosch A, Pulido-Leboeuf P, Gisbert J, Sanchez-Martos F, Vallejos A (2006) Geometry and dynamics of the freshwater-seawater interface in a coastal aquifer in southeastern Spain. Hydrol Sci J 51:543–555

Kacimov AR (2001) Analytical solution to a sharp interface problem in a vortex-generated flow. Water Resour Res 37:3387–3391

Kacimov AR (2002) Analytical solutions in a hydraulic model of seepage with sharp interfaces. J Hydrol 258:179–186

Kacimov AR (2006) Analytical solution and shape optimisation for groundwater flow through a leaky porous trough subjacent to an aquifer. Proc R Soc Lond A 462:1409–1423

Kacimov AR, Obnosov YuV (2001) Analytical solution for a sharp interface problem in sea water intrusion into a coastal aquifer. Proc R Soc Lond A 457:3023–3038

Kacimov AR, Youngs EG (2005) Steady-state water-table depressions caused by evaporation in lands overlying a water-bearing substratum. J Hydrol Eng ASCE 10(4):295–301

Kacimov AR, Obnosov Yu.V, Perret J (2004) Phreatic surface from a near-reservoir saturated tongue. J Hydrol 296:271–281

Kacimov AR, Obnosov Yu.V, Sherif MM, Perret J (2006) Analytical solution to a sea water intrusion problem with a fresh water zone tapering to a triple point. J Eng Math 54 (3):197–210. doi:10.1007/s10665-006-9030-9

Macumber PG (1998) The cable tool program and groundwater flow in the Eastern Batinah alluvial aquifer. Sultanate of Oman Ministry of Water Resources, Muscat, Oman

Ministry of Water Resources (1995) Eastern Batinah resource assessment. Progress Report N1. Sultanate of Oman Ministry of Water Resources, Muscat, Oman

Padilla F, Cruz-Sanjulian J (1997) Modeling sea-water intrusion with open boundary condition. Ground Water 35:704–709

Philip JR (1991) Upper bounds on evaporation losses from buried sources. Soil Sci Soc Am J 55:1516–1520

Polubarinova-Kochina PYa (1977) Theory of ground-water movement (in Russian). Nauka, Moscow

Segol G (1994) Classic groundwater simulations: proving and improving numerical models. Prentice Hall, Englewood Cliffs, NJ

Shammas M (2002) Seawater intrusion in Salalah aquifer, Oman. In: Sherif MM et al (ed) Environmental and groundwater pollution. Swets and Zeitlinger, Lisse, The Netherlands, pp 323–333

Sherif MM, Hamza KI (2001) Mitigation of seawater intrusion by pumping brackish water. Trans Porous Media 43:29–44

Sherif MM, Singh VP Amer AM (1988) A two dimensional finite element model for dispersion (2D-FED) in coastal aquifers. J Hydrol 103:11–36

Simunek J, Sejna M, van Genuchten M Th (1999) The HYDRUS-2D software package for simulating two-dimensional movement of water, heat, and multiple solutes in variably saturated media. Version 2.0, IGWMC-TPS-53, International Ground Water Modeling Center, Colorado School of Mines, Golden, CO, USA

Strack ODL (1989) Groundwater mechanics. Prentice Hall, Englewood Cliffs, NJ

Van Dam JC (1999) Exploitation, restoration and management. In: Bear J, Cheng A, Sorek S, Ouazar D, Herrera I (eds) Seawater intrusion in coastal aquifers concepts, methods and practices. Kluwer, Dordrecht, The Netherlands, pp 73–125

Van Der Veer P (1977) Analytical solution for steady interface flow in a coastal aquifer involving a phreatic surface with precipitation. J Hydrol 34:1–11

Verruijt A (1982) Theory of groundwater flow. Macmillan, London

Voss CI (1984) A finite-element simulation model for saturated-unsaturated, fluid-density dependent ground-water flow with energy transport or chemically-reactive single-species solute transport: US Geol Surv Water-Resour Invest Rep 81-4369, (rev. 1990), 409 pp

Voss CI (1999) USGS SUTRA code: history, practical use and application in Hawaii. In: Bear J, Cheng AHD, Sorek S, Ouzar D, Herrera I (eds) Seawater intrusion in coastal aquifers: concepts, methods, and practices: Kluwer, Dordrecht, the Netherlands, pp 249–313

Voss CI, Provost AM (2002) SUTRA, a model for saturated-unsaturated, variable density ground-water flow with solute or energy transport, US Geol Surv Water-Resour Invest Rept 02-4231, 105 pp

Weyhenmeyer CE, Burns SJ, Waber N, Macumber PG, Matter A (2002) Isotope study of moisture sources, recharge areas, and groundwater flow paths within the eastern Batinah coastal plain, Sultanate of Oman. Water Resour Res 38(10):1184, pp 2.1–2.22

Winston RB, Voss CI (2004) SutraGUI, a graphical user interface for SUTRA, a model for ground-water flow with solute or energy transport, US Geol Surv Open-File Rep 03-285, 114 pp
Wolfram S (1991) *Mathematica*: a system for doing mathematics by computer. Addison-Wesley, Redwood City, CA, USA
Wood WW, Sanford WE (2002) Hydrogeology and solute chemistry of the coastal-sabkha aquifer in the Emirate of Abu Dhabi. In: Barth H, Boer B (eds) Sabkha ecosystems, vol 1: the Arabian Peninsula and adjacent countries, Springer, Heidelberg, pp 173–185
Yechieli Y, Wood WW (2002) Hydrogeologic processes in saline systems: playas, sabkhas, and saline lakes. Earth Sci Rev 58:343–365
Youngs EG (2002) Maintaining fresh-water aquifers over saline water in coastal aquifers. J Agric Sci (Sultan Qaboos University)7:23–28

 DOI 10.1007/s10040-008-0425-8